



UNIVERSIDADE DA CORUÑA

FACULTAD DE CIENCIAS

Grado en Química

Memoria del Trabajo de Fin de Grado

*Estudio mediante Química Computacional de una
nanollave: reacciones de fotociclación/fotorreversión
on/off*

*Estudo mediante Química Computacional dunha
nanochave: reaccións de fotociclación/fotorreversión
on/off*

*Computational Chemistry Study of nano-keys:
photocyclization/photoreversion reactions on/off*

Director(es): ARTURO SANTABALLA LÓPEZ

MOISÉS CANLE LÓPEZ

SILVIA GARCÍA MONTEAGUDO

Curso: 2014/2015 – Convocatoria: *Septiembre*



Moisés Canle López, profesor titular de universidade, e J. Arturo Santaballa López, catedrático de universidade, ambos pertencentes o departamento de Química Física e Enxeñaría Química I (área de Química Física) da Universidade da Coruña

FAN CONSTAR

Que a presente memoria de traballo de fin de grao en Química titulada: “*Estudo mediante Química Computacional dunha nanochave: reaccións de fotociclación/fotorreversión on/off*” presentada pola graduada en Química dona Silvia García Monteagudo ten sido realizada baixo a nosa dirección, e considerando que cumpre tódalas condicións esixidas autorizámo-la súa presentación ante o tribunal correspondente.

Co gallo de que obre os efectos oportunos, asinámo-la presente o catorce de setembro de dous mil quince.

Asdo. Moisés Canle López

Asdo. J. Arturo Santaballa López

CONTENT

ABSTRACT	1
INTRODUCTION AND OBJECTIVES.....	4
BACKGROUND	8
DITHIENYLETHENES (DTEs)	9
ZERO POINT ENERGY (ZPE)	10
TRANSITION DIPOLE MOMENT	10
FRANCK-CONDON PRINCIPLE.....	11
RELAXATION MECHANISM FOR ELECTRONICALLY EXCITED MOLECULES	12
TRANSITION STRUCTURE	12
SINGLET–SINGLET ABSORPTION in solution	13
POPULATION ANALYSIS.....	15
MULLIKEN POPULATION ANALYSIS.....	15
METHODS.....	17
GEOMETRY OPTIMIZATION.....	18
SOLVATION MODELS	19
DENSITY FUNCTIONAL THEORY (DFT)	20
TIME-DEPENDENT DENSITY FUNCTIONAL THEORY (TD-DFT).....	20
CALCULATION OF EXCITATION AND EMISSION ENERGIES	21
CONVOLUTING UV-VIS SPECTRA USING OSCILLATOR STRENGTH	22
RESULTS AND DISCUSSION.....	25
MODEL COMPOUND (1).....	26
COMPOUND 3	35
SOLVENT EFFECTS.....	47
CONCLUSIONS	51

ABSTRACT

This work was focused on the study of organic photochromic compounds, dithienylethenes (DTEs), using computational chemistry methods. The density functional theory method (DFT) with 6-31G(d), as basis set, was used to study the ground state, and the conductor-like polarizable continuum model (CPCM) -implicit solvation model- was used to simulate solvents, mainly chloroform. Excitation and emission processes were studied using time-dependent density functional theory (TD-DFT). All calculations were carried out with the suite of programs Gaussian09.

Those quantum chemistry calculations allowed the study of geometries, kinetic, thermodynamic and photophysical parameters belonging to the closed and open forms (ground and excited states) of DTEs: [3-[thiophen-3-yl]-4-(thiophen-3-yl)-1*H* pyrrole-2,5-dione (**1**), [2-methylthiophen-3-yl]-4-(2-methylthiophen-3-yl)-1*H* pyrrole-2,5-dione (**2**) and 1-Benzyl-3-[2-methyl-5-(naphthalen-1-yl)thiophen-3-yl]-4-(2-methyl-5-phenylthiophen-3-yl)-1*H* pyrrole-2,5-dione (**3**)], and to their interconversion equilibria (closed \rightleftharpoons open).

The obtained results suggest the equilibrium is displaced towards the open form, the lower the electric permittivity of the solvent the higher the equilibrium constant. UV-Vis spectral results reasonably match the empirical observations. The presence of substituents increases the equilibrium constant (closed \rightleftharpoons open) several orders of magnitude.

Although it was not possible the calculation of the thermal transition state between the closed and the open form, a crude estimation of the activation energy suggests the photochemical nature of the ring opening/closure reaction of the studied dithienylethenes.

RESUMEN

Este trabajo se centró en el estudio de compuestos orgánicos fotocromicos, ditieniletanos (DTE), usando métodos de química computacional. El método de la teoría de densidad funcional (DFT), con 6-31G(d) como funciones base, fue empleado para estudiar el estado fundamental, y el modelo de conductor continuo polarizable (CPCM) –modelo de solvatación implícito- fue usado para simular disolventes, principalmente el cloroformo. Los procesos de excitación y emisión fueron estudiados usando la teoría de densidad funcional dependiente del tiempo (TD-DFT). Todos los cálculos se realizaron con el programa Gaussian09.

Estos cálculos de química cuántica han permitido estudiar la geometría, la cinética, las termodinámica y determinar los parámetros fotofísicos pertenecientes a las formas abierta y cerrada (estados fundamental y estado excitado) de los DTEs: [3-tiofen-3-il]-4-(tiofen-3-il)-1H pirrol-2,5-diona (**1**), [2-metiltiofen-3-il]-4-(2 metiltiofen-3-il)-1H pirrol-2,5-diona (**2**) y 1-bencil-3-[2-metil-5-(naftalen-1-il)tiofen-3-il]-4-(2-metil-5-feniltiofen-3-il)-1H pirrol-2,5-diona (**3**), y para su equilibrio de interconversión (cerrado \rightleftharpoons abierto).

Los resultados obtenidos sugieren que el equilibrio se desplaza hacia la forma abierta, y que a menor permitividad eléctrica del disolvente mayor es la constante de dicho equilibrio. Los resultados del espectro UV-VIS coinciden razonablemente con las observaciones empíricas. La presencia de los sustituyentes aumenta la constante de equilibrio (cerrada \rightleftharpoons abierta) varios órdenes de magnitud.

Aunque no fue posible calcular el estado de transición térmico entre la forma cerrada y abierta, una cruda estimación de la energía de activación confirma la naturaleza fotoquímica de la reacción de apertura/cierre en los compuestos ditieniletanos estudiados.

RESUMO

Este traballo centrouse no estudo de compostos orgánicos fotocromicos, ditieniletenos (DTE), usando métodos de química computacional. O método da teoría de densidade funcional (DFT), con 6-31G(d) como funcións base, foi usado para estudar o estado fundamental, e o modelo de condutor continuo polarizable (CPCM) –modelo de solvatación implícito- foi empregado para simular o disolvente, principalmente cloroformo. Os procesos de excitación e emisión foron estudados mediante a teoría de densidade funcional dependente do tempo (TD-DFT). Todos os cálculos foron levados a cabo usando o programa Gaussian09.

Os cálculos de química cuántica permitiron estudar a xeometría, a cinética, a termodinámica e determinar os parámetros fotofísicos pertencentes ás formas aberta e pechada (estados fundamental e excitados) dos DTEs: [3-tiofen-3-il]-4-(tiofen-3-il)-1H pirrol-2,5-diona (**1**), [2-metiltiofen-3-il]-4-(2 metiltiofen-3-il)-1H pirrol-2,5-diona (**2**) e 1-bencil-3-[2-metil-5-(naftalen-1-il)tiofen-3-il]-4-(2-metil-5-feniltiofen-3-il)-1H pirrol-2,5-diona (**3**), e para o seu equilibrio de interconversión (pechada \rightleftharpoons aberta).

Os resultados obtidos suxiren que o equilibrio desprazase cara a forma aberta, e que canto menor é a permitividade eléctrica do disolvente maior é a constante de equilibrio pechada \rightleftharpoons aberta. Os resultados dos espectros UV-VIS coinciden razoablemente coas observacións empíricas. A presenza de substituíntes aumenta a constante de equilibrio (pechada \rightleftharpoons aberta) en varios ordes de magnitude.

Aínda que non foi posible calcular o estado de transición térmico entre a forma pechada e aberta, unha crúa estimación da enerxía de activación confirma a natureza fotoquímica da reacción de apertura/peche nos compostos ditieniletenos estudados.

INTRODUCTION AND OBJECTIVES

During the last decade or so, the speed of the computers has grown considerably and the computational investigation of realistic models of organic compounds is becoming a standard practice. Quantum chemical methods are already capable of providing a complete description of what happens at the molecular level during bond-breaking and bond-forming processes. In particular, it is possible to compute the transition structure which connects a reactant to a product and the associated energy barrier with almost chemical accuracy.

A detailed understanding of the reaction pathway in the excited state manifold will increase our ability to design new and to control known photochemical reactions.

Photochemical processes, where the reactant resides on an excited state potential energy surface and the product accumulate on the ground state, could not be easily investigated. In photochemistry, the reaction path must have at least two branches: one located on the excited state and the other located on the ground state energy surface. The main difficulty associated with such computations lies in the correct definition and practical computation of the “funnel” region where the excited state reactant or intermediate is delivered to the ground state. During the last decade, computational tools have been developed and strategies discovered to explore electronically excited state reaction paths^{1,2,3,4}. The goal of such computational approaches, in the study of photochemical mechanisms, is the complete description of what happens at the molecular level from energy absorption to product formation.

The general objective of this work is to computationally study the photocyclization/photoreversion of dithienylethenes (DTEs). As first step is necessary to study the ground state and excited states of the corresponding open and closed forms. Therefore I will focus on the spectroscopic, kinetic and geometric characterization of the open and closed forms of 1-Benzyl-3-[2-methyl-5-(naphthalen-1-yl)thiophen-3-yl]-4-(2-methyl-5-phenylthiophen-3-yl)-1*H* pyrrole-2,5-dione in solution. To this end the specific objectives of this work are the following:

1. Determination of the optimum geometry of the open and closed forms
2. Determination of thermodynamic parameters of opening/closure process.

¹ A. Gilbert and J. Baggott, *Essentials of Molecular Photochemistry*, **1991**, Blackwell Scientific Publications

² J. Michl and V. Bonacic-Koutecky, *Electronic Aspects of Organic Photochemistry*, **1990**, Wiley

³ M. Klessinger and J. Michl, *Excited States and Photochemistry of Organic Molecules*, **1994**, VCH Publishers

⁴ B. O. Roos, in *Adv. Chem. Phys. (Ab Initio Methods in Quantum Chemistry-II)*, K. P. Lawley, **1987**, Ed., Wiley

3. Photophysical characterization of electronic transitions
4. Estimation of kinetic barrier for the opening/closure process.

Due to the complexity of the cited compound this study will start with a model compound: 3-[thiophen-3-yl]-4-(thiophen-3-yl)-1*H* pyrrole-2,5-dione (it what follows named as compound **1o** and its closed form **1c**) as it retains the main features of the initially proposed dithienylethene.

Calculations will also be carried out with: [2-methylthiophen-3-yl]-4-(2-methylthiophen-3-yl)-1*H* pyrrole-2,5-dione (**2o**) and its closed form (**2c**), and open and closed forms of 1-Benzyl-3-[2-methyl-5-(naphthalen-1-yl)thiophen-3-yl]-4-(2-methyl-5-phenylthiophen-3-yl)-1*H* pyrrole-2,5-dione (**3o** and **3c** respectively). The corresponding chemical structures are shown in Table 1.

Compound	Closed (c)	Open (o)
1		
2		
3		

Table 1. Chemical structures of studied molecules

The density functional theory method (DFT) with 6-31G(d) as basis set was used to study the ground state of those compounds and the Conductor-like Polarizable Continuum Model (CPCM) model was used to simulate solvents. Chloroform was the reference solvent as empirical data are reported using this solvent.

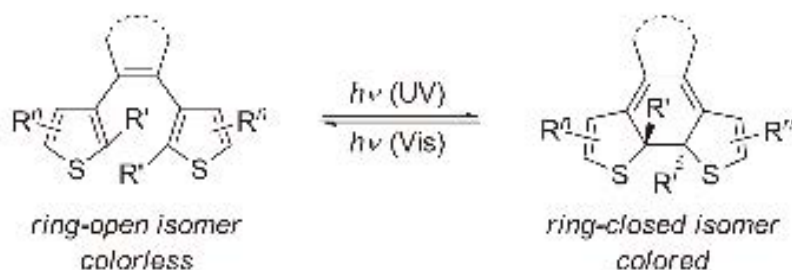
Excitation and emission processes were studied using time-dependent density functional theory (TD-DFT).

The suite of programs Gaussian 09 was used as implemented in the SVG computer of the Centro de Supercomputación de Galicia (CESGA); default values were always used.

BACKGROUND

DITHIENYLETHENES (DTEs)

Organic photochromic compounds have received increased interest due to their potential applications in optoelectronic molecular devices, such as molecular switches, logic gates, and information storage devices. Among the different families of photochromic materials, 1, 2-diarylethenes, in particular 1, 2-dithienylethenes (DTEs), which contain a cyclic ethylene bridge bound to two functionalized 2-substituted-3-thiophenyl moieties, are one of the most interesting due to their thermal stability and fatigue resistance. The molecular switching of DTEs is based on an efficient and reversible ON-OFF control photocyclization reaction between colourless ring-opened and coloured ring-closed isomers by selective irradiation.



Scheme 1. Photochromism of DTEs⁵.

Both isomeric forms of the DTEs show marked differences, not only in their absorption spectra, but also in other physical properties, such as the fluorescence intensity, redox potentials, refractive indices, dielectric constants, and geometric structure. The photochemical behaviour of these systems has been exploited in numerous fields, for example, the development of optical memory, optoelectronic devices, and organic semiconductors, the control of biological activity in living organisms, the direct conversion of light into mechanical work, or as molecular regulators in DNA interactions. All of these appealing applications have simulated the development of new synthetic approaches to prepare novel DTEs with selective functions.⁵

A very schematic view of the course of a photochemical reaction is that the system is promoted to an excited state ($R + h\nu \rightarrow R^*$). Photoproduct formation can then occur by adiabatic reaction ($R^* \rightarrow P'^*$) on the excited state (a photochemical process) followed by emission ($P'^* \rightarrow P'$) or by internal conversion to the ground state (a photo

⁵ Mosquera, A., Fernández, M.I., Canle, M., Pérez, J., Sarandeses, L.A. *Chem. Eur. J.* **2014**, *20*, 14524-14530.

physical process). The most common mechanism involves a non-adiabatic radiationless decay process which either regenerates the reactant R or generates new products P or P'.

Whether a photochemical reaction occurs, thus depends upon the relative rates of photochemical processes that generate new molecular structures versus competing photophysical processes that convert between electronic states at the same nuclear geometry.

ZERO POINT ENERGY (ZPE)

Also called quantum vacuum zero-point energy, is the lowest possible vibrational energy that a quantum mechanical physical system may have; it is the energy of this ground state.

TRANSITION DIPOLE MOMENT

Energy levels in matter are quantised, *i.e.* species can exist only in certain defined discrete energy states. A transition between two such states of specific energy must have associated with it a definite energy. Thus, a direct result of the quantisation of energy levels is that for each individual species only specific energies, and therefore frequencies, of radiation can be absorbed or emitted. The characteristic line and band spectra of chemical species are a consequence of this behaviour.

An oscillating electric or magnetic moment can be induced in an atom or molecule by electromagnetic radiation, such interaction is resonant if the frequency of the latter corresponds to the energy difference between the initial and final states of a transition. The amplitude of this dipole moment is referred to as the transition dipole moment, μ_{if} . It can be calculated as the integral taken over the product of the wavefunctions of the initial (i) and final (f) states of a spectral transition Ψ_i and Ψ_f and the dipole moment operator, ($\hat{\mu}$) of the electromagnetic radiation (Scheme 2).

$$\mu_{if} = \langle f | \mu | i \rangle = \int \Psi_f^* \hat{\mu} \Psi_i d\tau$$

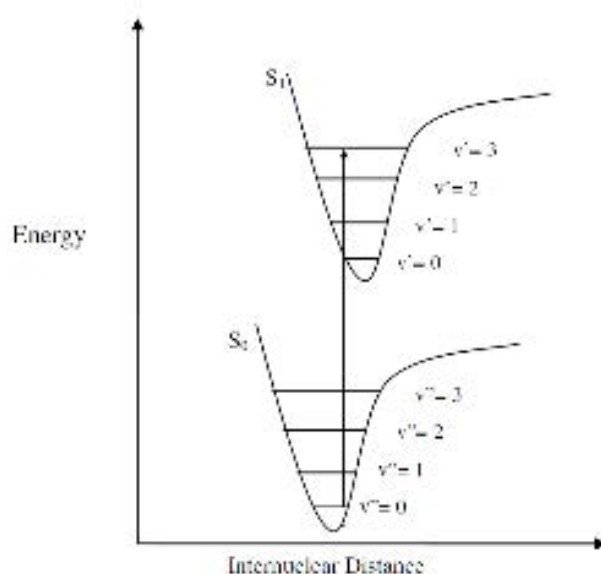
Scheme 2. Transition dipole moment⁶

⁶<http://core.ac.uk/download/pdf/279718.pdf> (Last accessed date: 09/09/2015)

The transition is allowed when the amplitude of the transition moment must be non-zero, leading to charge redistribution, its intensity being proportional to the square of the transition dipole moment.

FRANCK-CONDON PRINCIPLE

Nuclei are enormously heavy as compared to the electrons, during light absorption, which occurs in femtoseconds, electrons can move but not the nuclei. This result in a state known as the Franck-Condon state. The transition is vertical promoting the molecule from the lowest vibrational state (ZPE) of its electronic ground state (S_0) to a vibrational state of an electronically excited state (S_n).



Scheme 3. Franck-Condon principle for a diatomic molecule⁷

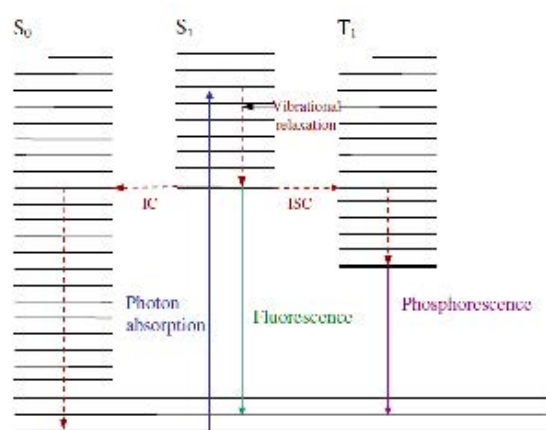
The vertical transition depicted in Scheme 3 occurs from the lowest vibrational energy level in the ground state (ZPE) to the vibrational energy level in the excited state that shows the greatest overlap integral of its wavefunction with that of the initial state, in this case, Scheme 3 shows the transition taking place from $v''=0$ (ZPE) to $v'=3$. This does not rule out other possible transition having also considerable overlap.

For polyatomic molecules, there are more transitions over a range of energies. The merging of these transitions leads to an absorption curve. This curve is described as the Franck-Condon envelope.

⁷ <http://core.ac.uk/download/pdf/279718.pdf> (Last accessed date: 09/09/2015)

RELAXATION MECHANISM FOR ELECTRONICALLY EXCITED MOLECULES

The absorption of radiation by a molecule results in most cases in the production of an electronically excited molecules that can exhibit different configuration and excess energy compared to the parent, ground state molecules. There are several routes by which the excited molecule can lose its excess energy and some of the most important routes are represented by a Perrin-Jablonski diagram.⁸



Scheme 4. Perrin-Jablonski diagram⁸

Since this work is not concerned with radiative processes such as fluorescence and phosphorescence, no further discussion of these processes will be undertaken.

TRANSITION STRUCTURE

A transition state is a particular configuration along the reaction coordinate in the framework of the transition state theory (TST). It is defined as the state corresponding to the highest potential energy along this reaction coordinate. At this point, assuming a perfectly irreversible reaction, colliding reactant molecules always go on to form products. It is often marked with the double dagger ‡ symbol.

A transition structure is the molecular species that is represented by the top of the potential energy curve in a simple one dimensional reaction coordinate diagram. The energy of this species is needed in order to determine the energy barrier to reaction and thus the reaction rate. The geometry of a transition structure is relevant for describing the reaction mechanism.

⁸ <http://core.ac.uk/download/pdf/279718.pdf> (Last accessed date: 09/09/2015)

SINGLET–SINGLET ABSORPTION IN SOLUTION

Steady-state spectroscopy is one of the most fundamental tools for investigating equilibrium structures and potential energy surfaces for different electronic states. However, interpreting such experimental data is often not straightforward. Density functional theory (DFT)^{9,10,11} and time-dependent DFT (TD-DFT)^{12,13,14,15,16,17} calculations are useful methods for studying them.

Most DFT computations use Becke's three-parameter hybrid functional¹⁸ with the Lee–Yang–Parr correlation functional (B3LYP)^{18,19,20} due to high correlation between theoretical and experimental data²¹. Usually only 'd'-polarization function is considered on heavy atoms to the standard 6-31G basis set²¹, since it is the best alternative to get satisfactory results with relatively low computational cost.

TD-DFT calculations including solvent effects could be performed using two different methods, that is, linear response (LR) and external iteration (EI) or state specific (SS) in older nomenclature^{22,23,24,25,26}. In the LR-PCM the excitation energies are "directly" determined without computing the exact excited electron density. In turn, in the EI-PCM approaches a different effective Schrödinger equation is solved for each state of interest, up to the fully variational formulation of solvent effect on the excited-state properties.

The dynamical solvent effect should also be considered during studying excited states in solution. Generally the total solvent polarization is always partitioned into two

⁹ Van Caillie, C., Amos, R.D., *Chem. Phys. Lett.* **1999**, 308, 249–255.

¹⁰ Gross, E.K.U., Dreizler, R.M. *Density Functional Theory*, Springer, Berlin, **1995**.

¹¹ Parr, R.G., Yang, W. *Density Functional Theory of Atoms and Molecules*, Oxford University Press, New York, **1989**.

¹² Bauernschmitt, R., Ahlrichs, R. *Chem. Phys. Lett.* **1996**, 256, 454–464.

¹³ Furche, F., Ahlrichs, R. *J. Chem. Phys.* **2002**, 117, 7433–7447.

¹⁴ Cossi, M., Barone, V., *J. Chem. Phys.* **2001**, 115, 4708–4717.

¹⁵ Casida, M.K. in: D.P. Chong (Ed.), *Recent Advances in Density Functional Methods. Part I*, World Scientific, Singapore, **1995**.

¹⁶ Casida, M.E., Jamorski, C., Casida, K.C., Salahub, D.R. *J. Chem. Phys.* **1998**, 108, 4439–4449.

¹⁷ Burke, K., Werschnik, J., Gross, E.K.U. *J. Chem. Phys.* **2005**, 123, 62206–62209.

¹⁸ Becke, A.D. *J. Chem. Phys.* **1993**, 98, 5648–5652.

¹⁹ Parr, R.G., Yang, W. *Ann. Rev. Phys. Chem.* **1995**, 46, 701–728.

²⁰ Lee, C., Yang, W., Parr, R.G. *Phys. Rev. B* **1988**, 37, 785–789.

²¹ Venkataramanan, N.S., Suvitha, A., Nejo, H., Mizuseki, H.Y. Kawazoe, *J. Quantum Chem.* 2011, 111, 2340–2351.

²² Cammi, R., Comi, S., Mennucci, B., Tomasi, J. *J. Chem. Phys.* 2005, 122, 104513.

²³ Comi, S., Cammi, R., Mennucci, B., Tomasi, J. *J. Chem. Phys.* **2005**, 123, 134512.

²⁴ Caricato, M., Mennucci, B., Tomasi, J., Ingrosso, F., Cammi, R., Comi, S., Scalmani, G. *J. Chem. Phys.* **2006**, 124, 24520.

²⁵ Improta, R., Barone, V., Scalmani, G., Frisch, M.J. *J. Chem. Phys.* **2006**, 125, 054103.

²⁶ Improta, R., Scalmani, G., Frisch, Barone, V. *J. Chem. Phys.* **2007**, 127, 074504.

degrees of freedom, ‘slow’ and ‘fast’^{25,26}. The ‘slow’ part can be regarded as the reorganization of the solvent molecules as a response to a change in the electronic density of the solute. The ‘fast’ part can be regarded as the response of the electrons in the solvent to a change in the electronic density of the solute. In an equilibrium (EQ) solvation calculation, both components are in equilibrium with the electron density of the excited-state density. Additionally, the solvent reaction field depends on the static dielectric constant of the medium.

In turn, in a non-equilibrium (NEQ) only solvent electronic polarization connected with ‘fast’ degree of freedom is in equilibrium with the excited-state electron solute’s density. Moreover, the ‘slow’ solvent components remain equilibrated with the ground-state electron density.

In LR-PCM solvent degrees of freedom are always equilibrated with the ground-state density. Therefore, a single-point LR-PCM/ TD-DFT calculation for absorption and emission energies are performed defaults to non-equilibrium solvation. EI-PCM/TD-DFT excitation energy calculations are performed by solving the ‘fast’ components (‘slow’ component comes from the origin state) of the solvent polarization self-consistently with the selected excited-state density. This description shows EI-PCM approach provides a more rigorous treatment of dynamical solvent effect than LR-PCM. Moreover, LR-PCM calculations have been shown to overestimate solvent effects on the intensities of particular bands^{25,26}. The two other limitations of this method are connected to the treatment of the emission processes and the study of the electronic transitions involving a substantial electron density shift^{25,26}. In turn, EI-PCM methods provide a balanced description of strong and weak electronic transitions and give accurate estimates of dynamical solvent effect on the absorption and fluorescence emission processes. Therefore, vertical excitation energy from the result of LR/TD-DFT geometry optimizations should be supplement by single-point EI/TD-DFT calculations.

Chloroform solution has been used as a solvent in calculations. The effects of solvent, substrate, and electric field have been considered using a polarized continuum model (PCM)^{27,28,29,30,31,32,33}. In order to characterize singlet–singlet absorption features the LR and EI approaches have been used.

²⁷ Cossi, M., Barone, V. *J. Chem. Phys.* **2000**, 112, 2427–2435.

²⁸ Cossi, M., Barone, V., Cammi, R., Tomasi, J. *Chem. Phys. Lett.* **1996**, 255, 327–335.

²⁹ Barone, V., Cossi, M., J. Tomasi, J. *J. Comput. Chem.* **1998**, 19, 404–417.

POPULATION ANALYSIS

Can be used to calculate atom partial charges, which allows to partition electronic density or wavelength function, in localized charges on nucleus. Mulliken population analysis does not reflect electronegativity on involved atoms, and suggest that two orbitals overlap is equivalently shared.

MULLIKEN POPULATION ANALYSIS

The Mulliken approach to the calculation of atomic charges³⁴ takes as a starting point the observation that the wave function, and thus the charge density, is expanded in basis functions attached to the atomic nuclei. In an atomic basis-set expansion, the charge distribution ρ may be written as:

$$\rho = \sum_{kl} D_{kl} \chi_k \chi_l$$

where \mathbf{D} is the density matrix and χ a basis function. The indices k and l run over all basis functions of the system. The summation may be restricted over k to basic functions at nucleus K and the summation over l to basic functions at nucleus L. Integrating over the physical space, a charge q_{KL} assigned to the two nuclei K and L may then be written as

$$q_{KL} = \sum_{k \in K} \sum_{l \in L} D_{kl} S_{kl} = \sum_{k \in K} \sum_{l \in L} q_{kl}$$

where \mathbf{S} is the one-electron overlap matrix and q_{kl} a charge assigned to the two basic functions χ_k and χ_l . If $k = l$, q_{kk} is trivially assigned to nucleus K. For the multicentre charges the situation is less clear. Mulliken originally assigned one-half of q_{kl} to nucleus K and the other half to nucleus L, but other schemes have also been proposed. Some of these schemes have been generalized to higher-order atomic moments by replacing the overlap matrix in the previous equation with for example the dipole-moment matrix.³⁵ The reliability of Mulliken charges has been discussed extensively, in particular their dependence on the basis set.³⁶

³⁰ Tomasi, J., Mennucci, B., Cammi, R. *Chem. Rev.* **2005**, 105, 2999–3093.

³¹ Mennucci, B., Cammi, R. *Continuum Solvation Models in Chemical Physics: From Theory to Applications*, Wiley, New York, **2007**.

³² Tomasi, J., Mennucci, B., Cancès, E. *J. Mol. Struct. (Theochem)* **1999**, 464, 211–226.

³³ Foresman, J.B., Keith, T.A., Wiberg, K.B., Snoonian, J., Frisch, M.J. *J. Phys. Chem.* **1996**, 100, 16098–16104.

³⁴ Mulliken, R. S. *J. Chem. Phys.* **1955**, 23, 1833.

³⁵ Vigné-Maeder, F.; Claverie, P. *J. Chem. Phys.* **1988**, 88, 4934.

³⁶ Stone, A. J. *The theory of intermolecular forces*; Clarendon Press: Oxford, 1996.

It should be noted that the electrostatic interaction energies calculated with atomic moments in a Mulliken-type scheme are much less sensitive to the basis set than are the atomic moments themselves.³⁷ The reason for this behaviour appears to be that the atomic moments by definition give the correct molecular moments to the same order as the expansion of the atomic moments and low-order atomic moments seem to give accurate higher-order molecular moments.

For larger molecules, the atomic charges may be derived from fits to the quantum-chemically derived electrostatic potential and field around the molecule, to the potential and field obtained from a distributed multipole expansion, or to the molecular electric moments.³⁸

³⁷ Stone, A. J.; Alderton, M. *Mol. Phys.* **1985**, *56*, 1047-1064.

³⁸ Dinur, U. Hagler, A. T. *J. Comp. Chem.* **1995**, *16*, 154-170.

METHODS

GEOMETRY OPTIMIZATION

The potential energy surface (PES) specifies the way in which the energy of a molecular system varies with small changes in its structure. In this way, a potential energy surface is a mathematical relationship linking the molecular structure and the resultant energy.

For a diatomic molecule, the potential energy surface can be represented by a two dimensional plot with the internuclear separation on the X-axis and the energy at that bond distance on the Y-axis; for larger systems the surface is multidimensional.

A typical bidimensional PES contains three stationary points: two minima (a minimum is a point at the bottom of a valley) from which motion in any direction leads to a higher energy, and one saddle point, the transition structure, at which any direction leads to a higher energy but those directed to both minima.

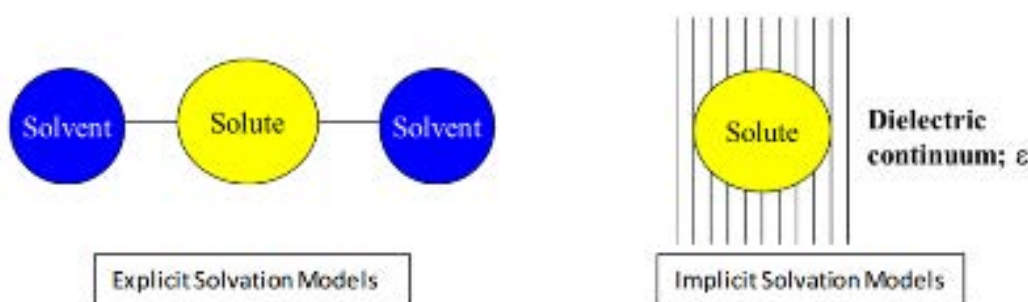
Performing a geometry optimization is usually the first step to study a molecule using computational methods. Geometry optimizations typically attempt to locate stationary points on the potential energy surface in order to predict equilibrium structures of molecular systems.

At both minima and saddle points, the first derivative of the energy, known as the gradient, is zero. Since the gradient is the negative of the forces, the forces are also zero at such points, this is the reason because they are called stationary points. All successful optimizations locate a stationary point, although not always the one that was intended. Geometry optimizations usually locate the stationary point closest to the geometry from which they started.

When performing a minimization, intending to find the minimum energy structure a local minimum or a saddle point can be found. A geometry optimization alone cannot establish the nature of the stationary point that it finds. In order to characterize a stationary point, it is necessary to perform a frequency calculation on the optimized geometry. Frequency calculations will include a variety of results: frequencies, intensities, the associated normal modes, the structure's zero point energy, and various thermo-chemical properties. If there is only one negative frequency, such frequency is known as imaginary frequency and corresponds to a saddle point; on the other hand, when all the frequency values are positive such stationary point corresponds to a minimum in the PES.

SOLVATION MODELS

The interactions between the solvent and the solute impact the chemistry of the molecule being studied. The interaction can vary energy, stability, and molecular orientation, and as a consequence energy related properties will also change. Therefore a way to model the chemistry of these molecules in a solvent is required. This is accomplished using implicit solvation models (Scheme 5). These models differ from the explicit ones because in the way they treat solvent. Explicit models deal with the solvent as individual molecules; meanwhile implicit models treat the solvent as a continuous medium that acts upon the solute. This leads to a significant reduction in complexity by describing the solvent as a uniform continuum than having to calculate multiple molecular interactions.



Scheme 5. Explicit and implicit solvation models³⁹

There are many models, the one that was used in the present calculations is Conductor-like Polarizable Continuum Model (CPCM), the most commonly employed model for implicit solvation, is a variation of the DPCM model in that it used a group of nuclear centred spheres to define the cavity within a dielectric continuum. The difference between both models is that de CPCM model treats the solvent like a conductor. This fact impacts the polarization charges of the accessible surface area between the solvent and the solute. The CPCM model attempts to solve the nonhomogeneous Poisson equation for an infinite dielectric constant with scaled dielectric boundary conditions to approximate the result for a finite dielectric constant.

In the CPCM model the permittivity will behave more like an ideal conductor and return better results. This model also differs from DPCM model in that it reduces the outlying charge errors which are the errors caused by portions of the electron density which are actually outside the cavity.

³⁹ http://www.uwyo.edu/kubelka-chem/implicit_solvent_models.pdf (Last accessed date: 09/09/2015)

The reason why this model is used is because math involved in calculating the free energy of solvation gets simpler. That's because dielectric continuum is considered as a conductor-like continuum, the dielectric constant is infinite and polarizability of the system becomes zero with a conductor like solvent. Computational cost decreased. Finally the high quality of the results for high permittivity solvent makes this model adequate for this work, although I have in mind that this method is not perfect.⁴⁰

DENSITY FUNCTIONAL THEORY (DFT)

The density functional theory (DFT) is presently the most successful and also the most promising approach to compute the electronic structure of matter. Its applicability ranges from atoms, molecules and solids to nuclei and quantum and classical fluids. In its original formulation, the density functional theory provides the ground state properties of a system, and the electron density plays a key role.

A functional is a function of a function. In DFT the functional is the electron density which is a function of space and time.¹¹ The electron density is used in DFT as the fundamental property unlike Hartree-Fock theory which deals directly with the many-body wavefunction. Using the electron density significantly speeds up the calculation. Whereas the many-body electronic wavefunction is a function of $3N$ variables (the coordinates of all N atoms in the system) the electron density is only a function of x, y, z -only three variables. Hohenberg and Kohn stated a theorem which tells us that the electron density is very useful. The Hohenberg-Kohn theorem asserts that the density of any system determines all ground-state properties of the system.¹¹ In this case the total ground state energy of a many-electron system is a functional of the density. So, if the electron density functional is known, also is the total energy of the system and it is possible the calculation of related properties.

TIME-DEPENDENT DENSITY FUNCTIONAL THEORY (TD-DFT)

Over the past decade, time-dependent density functional theory (TD-DFT)⁴¹ has become one of the most prominent methods for calculating excited states.⁴² A major advantage of TD-DFT is its low computational cost,⁴³ roughly comparable with single excitation theories based on the Hartree-Fock (HF) ground state such as configuration

⁴⁰ http://www.uwo.edu/kubelka-chem/implicit_solvent_models.pdf (Last accessed date: 09/09/2015)

⁴¹ Runge, E., Gross, E. K. U. *Phys. Rev. Lett.* **1984**, *52*, 997.

⁴² Dreuw, A., Head-Gordon, M. *Chem. Rev.* **2005**, *105*, 4009.

⁴³ Bauernschmitt, R., Ahlrichs, R. *Chem. Phys. Lett.* **1996**, *256*.

interaction with singles or the random phase approximation. TDDFT excitation energies are computed as poles of the frequency-dependent density matrix response.⁴¹ Since the commonly used adiabatic approximation represents this response in terms of single excitations, TD-DFT is best suited for excited states that are dominated by single excitations. TD-DFT properties are obtained from derivatives of the excited-state energy with respect to external perturbations.^{44,45} TD-DFT calculations can be standardized and no need to define an active space or to select reference configurations.

CALCULATION OF EXCITATION AND EMISSION ENERGIES

Geometry optimizations and absorption/emission calculations were carried out at B3LYP/6-31G (d) level using Gaussian 09 software.⁴⁶

Polarizable Continuum Model (PCM) calculations were performed to find excitation and emission energies.

These steps were followed for excitation calculations in solution:

- 1) Optimize ground state using keyword SCRF. This gives ground state optimized geometry with solvent equilibrated.
- 2) A TDDFT calculation is performed to find excited states at ground state equilibrium geometry. Solvent is not equilibrated with respect to excited states. This step assumes linear response of the solvent to excited state. Solvent effects are not accurately accounted in this step. State specific solvation (SS) method is followed after this step for describing solvent effects.
- 3) Self consistent calculation is done to consider interaction of solvent and excited state electron density of the molecule. These calculations are called as state specific calculation since; it assumes interaction of particular excited state with the solvent.

Emission calculations were done using following procedure:

⁴⁴ Furche, F., Ahlrichs, R. *J. Chem. Phys.* **2002**, *117*, 7433.

⁴⁵ Furche, F., Ahlrichs, R. *J. Chem. Phys.* **2004**, *121*, 12772.

⁴⁶ Gaussian 09, Revision **D.01**, Frisch, M. J.; Trucks, G. W.; Schlegel, H. B.; Scuseria, G. E.; Robb, M. A.; Cheeseman, J. R.; Scalmani, G.; Barone, V.; Mennucci, B.; Petersson, G. A.; Nakatsuji, H.; Caricato, M.; Li, X.; Hratchian, H. P.; Izmaylov, A. F.; Bloino, J.; Zheng, G.; Sonnenberg, J. L.; Hada, M.; Ehara, M.; Toyota, K.; Fukuda, R.; Hasegawa, J.; Ishida, M.; Nakajima, T.; Honda, Y.; Kitao, O.; Nakai, H.; Vreven, T.; Montgomery, J. A., Jr.; Peralta, J. E.; Ogliaro, F.; Bearpark, M.; Heyd, J. J.; Brothers, E.; Kudin, K. N.; Staroverov, V. N.; Kobayashi, R.; Normand, J.; Raghavachari, K.; Rendell, A.; Burant, J. C.; Iyengar, S. S.; Tomasi, J.; Cossi, M.; Rega, N.; Millam, J. M.; Klene, M.; Knox, J. E.; Cross, J. B.; Bakken, V.; Adamo, C.; Jaramillo, J.; Gomperts, R.; Stratmann, R. E.; Yazyev, O.; Austin, A. J.; Cammi, R.; Pomelli, C.; Ochterski, J. W.; Martin, R. L.; Morokuma, K.; Zakrzewski, V. G.; Voth, G. A.; Salvador, P.; Dannenberg, J. J.; Dapprich, S.; Daniels, A. D.; Farkas, Ö.; Foresman, J. B.; Ortiz, J. V.; Cioslowski, J.; Fox, D. J. Gaussian, Inc., Wallingford CT, 2009.

- 1) Excited state is optimized, with linear response from solvent. This optimization is carried using TDDFT method, since, excited state calculation is done. Minimum energy geometry on the excited state under consideration is found.
- 2) State specific equilibrium solvation of excited state at corresponding equilibrium geometry is carried. Then solvation data at this step is written in PCM inputs for next step. This step is necessary to achieve equilibrium of solvent-molecule system for fast and slow degrees of freedom. Usually, electron density is treated as fast degree of freedom which adjusts instantaneously on excitation of molecule. Slow degree often refers to nuclear motion.
- 3) Ground state energy calculation at excited state geometry is done. Static solvation at excited state is read from PCM inputs written in last step.

CONVOLUTING UV-VIS SPECTRA USING OSCILLATOR STRENGTH⁴⁷

In general, the absorption or emission of light by a chemical compound is accompanied by a transition of states. The energy difference between these states ΔE is related to the frequency ν , the wavelength λ and the wave number $\bar{\nu}$ of absorbed or emitted light as follows:

$$\Delta E = h\nu = \frac{hc}{\lambda} = hc\bar{\nu}$$

where h is Planck's constant and c is the speed of light.

The absorption of light by a compound in solution is defined as:

$$A = \log \frac{I_0}{I}$$

this absorption is proportional to the concentration, C , and the path-length (e.g. width of the cuvette), l . This is the Beer-Lambert Law $A = \varepsilon \cdot C \cdot l$ where the constant of proportionality ε is referred to as the decadic molar absorption coefficient, or simply the molar absorptivity.

The absorptivity is a measure of the intensity of an electronic transition and how strongly it is allowed. Experimentally, bands are observed and the overall strength of an electronic transition must be evaluated by integrating over the associated band.

Next we introduce the concept of the oscillator strength of a particular electronic transition. This dimensionless quantity is defined as follows:

⁴⁷ <http://gausssum.sourceforge.net/DocBook/ch07.html> (Last accessed date: 05/09/2015)

$$f = \frac{4m_e c \epsilon_0}{N_A e^2} B$$

where m_e is the mass of an electron, ϵ_0 the vacuum permittivity, N_A Avogadro's constant, e the elementary charge and B the molar natural absorption coefficient integrated over the whole band in units of frequency (from ν_1 to ν_2). The oscillator strength is a number usually between one and zero. Forbidden transitions have oscillator strengths close to zero, while bands arising from electronically allowed transitions show values of the order of one.

Rearrangement of B into terms already introduced yields:

$$B = \int_{\nu_1}^{\nu_2} \frac{\ln \frac{I}{I_0}}{Cl} \cdot d\nu = \ln 10 \int_{\nu_1}^{\nu_2} \epsilon \cdot d\nu = c \ln 10 \int_{\bar{\nu}_1}^{\bar{\nu}_2} \epsilon \cdot d\bar{\nu}$$

and substituting into the previous equation gives:

$$f = \frac{4m_e c^2 \epsilon_0}{N_A e^2} \ln 10 \int_{\bar{\nu}_1}^{\bar{\nu}_2} d\bar{\nu} \cdot \epsilon$$

Theoretically (under the transition dipole length approximation), the oscillator strength can be related to the transition dipole moment, \mathbf{M} , as follows:

$$f_{i \rightarrow f} = \frac{8\pi^2 m_e}{3e^2 h^2} \Delta E_{i \rightarrow f} |M_{i \rightarrow f}|^2 = \frac{8\pi^2 m_e c}{3e^2 h^2} \bar{\nu}_{i \rightarrow f} |M_{i \rightarrow f}|^2$$

then Gaussian functions are used to convolute calculated oscillator strengths for comparison with experimental results. Gaussian functions $g(x)$ are of the general form:

$$g(x) = N \cdot e^{-\alpha(x-\beta)^2}$$

they are centred at β , which can easily be shown by substituting $x = \beta$, yielding the maximum value $g(\beta) = N$. Their integral over the whole of space is:

$$\int_{-\infty}^{\infty} g(x) dx = N \sqrt{\frac{\pi}{\alpha}}$$

the shape of the band profile is approximated as a Gaussian function $g(x) = \epsilon(\bar{\nu})$, *i.e.* the decadic molar absorption coefficient as a function of wave number. Combining previous equations, we get:

$$\int_{-\infty}^{\infty} \epsilon(\bar{\nu}) d\bar{\nu} = N \sqrt{\frac{\pi}{\alpha}} = \frac{N_A e^2 f}{4m_e c^2 \epsilon_0 \ln 10}$$

Now introducing the parametrical value of the full-width half-maximum (FWHM) of the band given in units of $\bar{\nu}$ and symbolised by $\Delta_{1/2}\bar{\nu}$. Solving for this value by substituting $\varepsilon(\beta \pm \frac{1}{2}\Delta_{1/2}\bar{\nu}) = \frac{1}{2}N$ we obtain:

$$\alpha = \frac{4\ln 2}{(\Delta_{1/2}\bar{\nu})^2}$$

with α we can now solve for the normalisation constant N obtaining:

$$N = \frac{N_A e^2 f}{2m_e c^2 \epsilon_0 \ln 10 (\Delta_{1/2}\bar{\nu})} \sqrt{\frac{\ln 2}{\pi}}$$

Substituting these results with $\beta = \bar{\nu}_{i \rightarrow f}$ and simplifying the constants into numerical expressions gives us:

$$\varepsilon(\bar{\nu}) = \frac{2.175 \cdot 10^8 \text{ L} \cdot \text{mol}^{-1} \cdot \text{cm}^{-2}}{\Delta_{1/2}\bar{\nu}} \cdot f \cdot e^{\left[-2.772 \left(\frac{\bar{\nu} - \bar{\nu}_{i \rightarrow f}}{\Delta_{1/2}\bar{\nu}}\right)^2\right]}$$

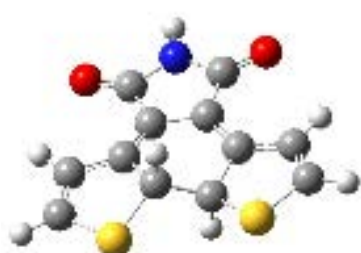
The value of full-width half-maximum (FWHM) of the band ($\Delta_{1/2}\bar{\nu}$) should be supplied while the values of the oscillator strength (f) and $\bar{\nu}_{i \rightarrow f}$ are obtained from quantum mechanical calculations.

RESULTS AND DISCUSSION

MODEL COMPOUND (1)

Geometry optimization of **1c** (closed) and **1o** (open) was carried out at B3LYP/6-31G (d) level using Gaussian 09 software. The Polarizable Continuum Model (PCM) calculations were performed to find excitation and emission energies. The nature of the stationary points as minima was confirmed by checking all vibrational frequencies values were positive.

As it was stated in the introduction chapter, the relative complexity of the initial compound suggested carrying out the first part of this computational study with the following simpler pair of model compounds:



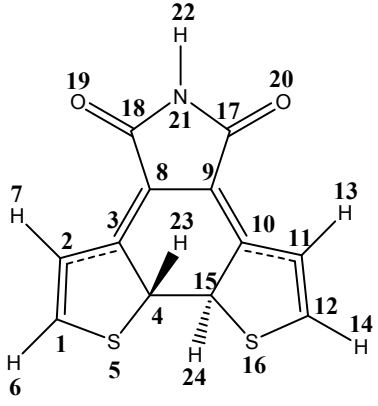
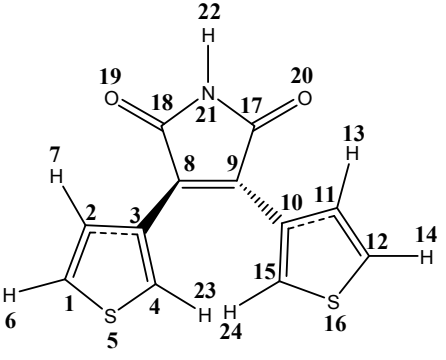
1c



1o

Selected atomic distances and bond lengths are collected in Table 2, whereas angles are shown in Table 3, and dihedral angles in Table 4.

Table 2. Atom numbering and selected atomic distances and bond lengths of closed and open forms

					
Closed	Distance / Å	Open	Closed	Distance / Å	Open
1.360	C3-C8	1.463	1.549	C15-C4	3.296
1.452	C8-C9	1.364	1.880	S16-C15	1.724
1.360	C9-C10	1.463	3.099	H23-H24	2.817
1.541	C10-C15	1.380			

Most distances remain equal within $\pm 0.03 \text{ \AA}$, larger changes appear in Table 2; they come from the C4-C15 bond breaking, which is accompanied by the change in bond orders due to the corresponding electronic rearrangement.

Table 3. Atom numbering and selected angles of closed and open forms.

Closed	Angle / $^{\circ}$	Open
130.4	C2-C3-C8	123.8
130.4	C9-C10-C11	123.8
117.0	C4-C3-C8	124.6
117.0	C15-C10-C9	124.6
109.4	C3-C4-C15	84.2
109.4	C10-C15-C4	84.2
122.0	C3-C8-C9	131.9
122.0	C8-C9-C10	131.9
107.6	C3-C4-H23	123.9
107.6	C10-C15-H24	127.8
104.1	C10-C15-S16	112.2
104.1	C3-C4-S5	112.2

As shown in Table 2 many bond angles of **1c** and **1o** are similar within $\pm 3^{\circ}$, again major changes take place in the atoms corresponding to the ring being broken.

Main geometrical difference between the open and closed form of **1** comes from the observation of dihedral angles (Table 3). Due to the C5-C15 bond breaking a restructuring of many dihedral angles takes place, the ones who changes most are the ones belonging to the central ring.

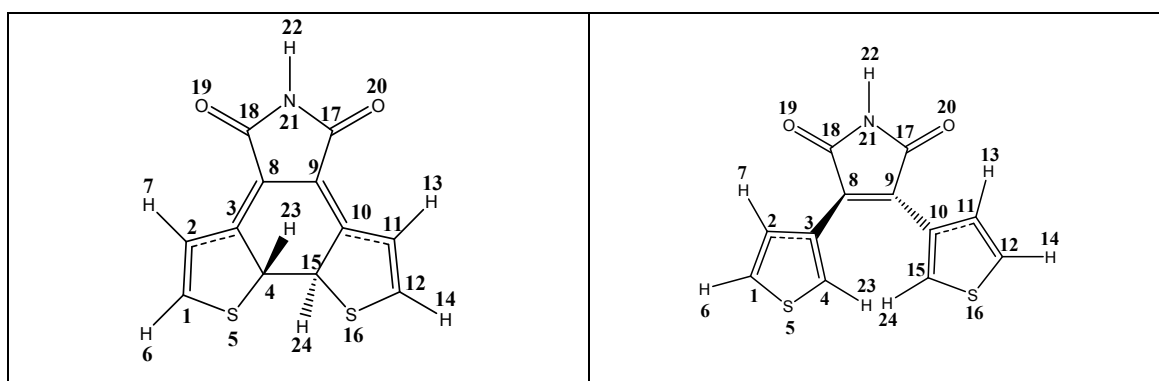
Table 4. Atom numbering and selected dihedral angles of closed and open forms

Closed	Dihedral angle / °	Open
-13.4	C1-C2-C3-C4	-0.7
-13.4	C12-C11-C10-C15	-0.7
18.4	C2-C3-C4-S5	0.3
18.4	C11-C10-C15-S16	0.3
7.7	C4-C3-C8-C9	31.8
7.7	C15-C10-C9-C8	31.8
18.9	C4-C8-C9-C15	36.9
83.3	C8-C3-C4-H23	-2.2
83.3	C9-C10-C15-H24	-1.4
10.3	C3-C8-C9-C10	8.0
174.5	H23-C4-C15-H24	144.6

The central ring breakage implies electronic rearrangement, changes in the hybridization of several bonds which mainly affects to dihedral angles. Ring opening is accompanied by loss of planarity, in this way steric effects are minimized.

The change in charge is collected in Table 5. Those atomic charges were calculated according to the Mulliken approach.³⁴ Many atoms bear similar charges in both model compounds (**1c** & **1o**), whereas there are noticeable changes in others. The change occurs not only in the atoms involved in the central ring, sulphur and even oxygen atoms show large differences in their atomic charge when **1c** and **1o** are considered. The similarity of the charges of C8 and C15 is somehow surprising.

Table 5. Atom numbering and Mulliken charges of closed and open forms



Closed /Mulliken	Charge	Open / Mulliken
-0.323	C1	-0.369
-0.084	C2	-0.096
0.021	C3	0.075
-0.338	C4	-0.379
0.186	S5	0.272
0.211	H6	0.199
0.184	H7	0.172
-0.001	C8	-0.278
-0.001	C9	-0.276
0.021	C10	0.075
-0.084	C11	-0.964
-0.323	C12	-0.367
0.184	H13	0.171
0.211	H14	0.200
-0.338	C15	-0.374
0.186	S16	0.272
0.600	C17	0.611
0.600	C18	0.611
-0.530	O19	-0.502
-0.530	O20	-0.501
-0.690	N21	-0.684

Energy terms related to the first $S_0 \rightarrow S_n$ absorptions and to $S_1 \rightarrow S_0$ emission of **1c** and **1o** are listed in Tables 6 and 7 respectively.

Table 6. Energy terms related to the $S_0 \rightarrow S_n$ absorption of the closed and open forms of **1**

1

Absorption $S_0 \rightarrow S_n$ (closed form)						
Term	$\Delta E_{ve} /$	$\Delta E_{ve} (SS) /$	$\Delta E_{ad} /$	$\Delta E_{00} /$	$\Delta E_{reorg} /$	$\Delta E_{reorg} (SS) /$
Transition	nm eV	nm eV	nm eV	nm eV	$\text{kJ}\cdot\text{mol}^{-1}$	$\text{kJ}\cdot\text{mol}^{-1}$
$S_0 \rightarrow S_1$	479.7	465.8	575.9	598.3	385.2	377.8
	2.58	2.66	2.15	2.07		
$S_0 \rightarrow S_2$		398.6	414.9	423.6		417.0
		3.11	423.6	2.93		
Absorption $S_0 \rightarrow S_n$ (open form)						
Term	$\Delta E_{ve} /$	$\Delta E_{ve} (SS) /$	$\Delta E_{ad} /$	$\Delta E_{00} /$	$\Delta E_{reorg} /$	$\Delta E_{reorg} (SS) /$
Transition	nm eV	nm eV	nm eV	nm eV	$\text{kJ}\cdot\text{mol}^{-1}$	$\text{kJ}\cdot\text{mol}^{-1}$
$S_0 \rightarrow S_1$	456.3	494.4	544.0	553.0	382.6	402.8
	2.72	2.51	2.28	2.24		
$S_0 \rightarrow S_2$		428.9	418.0	422.3		432.8
		2.89	2.97	2.94		

Table 7. Energy terms related to the $S_1 \rightarrow S_0$ emission of the closed and open forms of **1**

Emission $S_0 \rightarrow S_1$ (closed form)			Emission $S_0 \rightarrow S_1$ (open form)		
Term	$\Delta E_{em} (SS) /$	$\Delta E_{reorg} (SS) /$	Term	$\Delta E_{em} (SS) /$	$\Delta E_{reorg} (SS) /$
Transition	$\text{kJ}\cdot\text{mol}^{-1}$ nm eV	$\text{kJ}\cdot\text{mol}^{-1}$	Transition	$\text{kJ}\cdot\text{mol}^{-1}$ nm eV	$\text{kJ}\cdot\text{mol}^{-1}$
$S_1 \rightarrow S_0$	164.5	35.4	$S_1 \rightarrow S_0$	151.3	65.1
	727.2			790.9	
	1.71			1.57	

The meaning of the energy terms of Tables 6 and 7 are illustrated in the following figure:

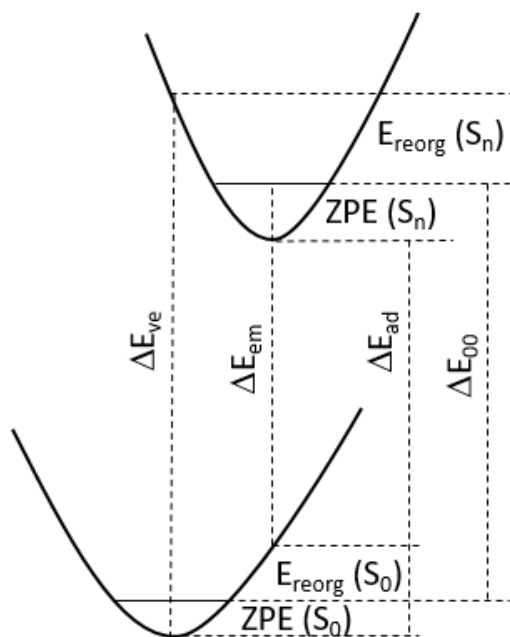



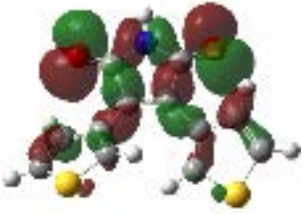
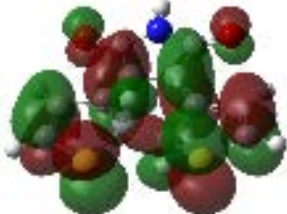



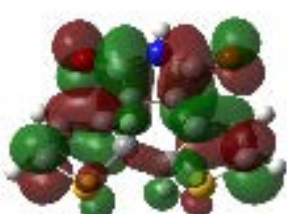
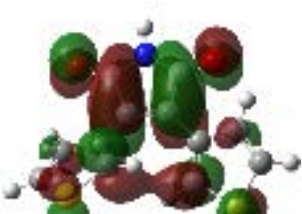
Figure 1. Energy terms involved in the absorption-emission process

From Table 6 it follows that the vertical excitation taking properly into account the solvent reorganization (ΔE_{ve} (SS)) is higher for the closed form, the contrary happens for the adiabatic and 00 energies (ΔE_{ad} and ΔE_{00}). Regarding the reorganization energy in the excited state (ΔE_{reorg} (SS)), *i.e.* the relaxation from the arriving level to the zero point energy of the excited state, more energy is lost of the open form. The same applies to the $S_0 \rightarrow S_2$ absorption. It is noticeable the inversion of the trend when the corresponding energy terms, ΔE_{ve} and ΔE_{reorg} , do not include the solvent reorganization in the arriving state.

According to Table 7 the emission energy (ΔE_{em} (SS)) is higher in the case of the closed form, whereas the opposite occurs to the reorganization energy within the ground state (ΔE_{reorg} (SS)).

Table 8 shows the frontier orbitals, HOMO and LUMO, and inner orbitals with major contributions to the two lowest singlet-singlet transitions of the closed and open forms of **1**. The similarity of the values for the $S_0 \rightarrow S_1$ (Table 6) is consistent with the transition involving HOMO and LUMO.

Table 8. Frontier and inner orbitals involved in the two lowest excitations

	Closed		Open	
HOMO-1			HOMO-4	
HOMO			HOMO-1	
LUMO			HOMO	
LUMO+1			LUMO	
$S_0 \rightarrow S_1$	HOMO \rightarrow LUMO		$S_0 \rightarrow S_1$	HOMO \rightarrow LUMO
$S_0 \rightarrow S_2$	HOMO-1 \rightarrow LUMO HOMO \rightarrow LUMO+1		$S_0 \rightarrow S_2$	HOMO-1 \rightarrow LUMO HOMO-4 \rightarrow LUMO

Individual contribution of the most intense ten transitions to the UV-VIS spectrum of **1o** and **1c** is shown in Figures 2 & 3.

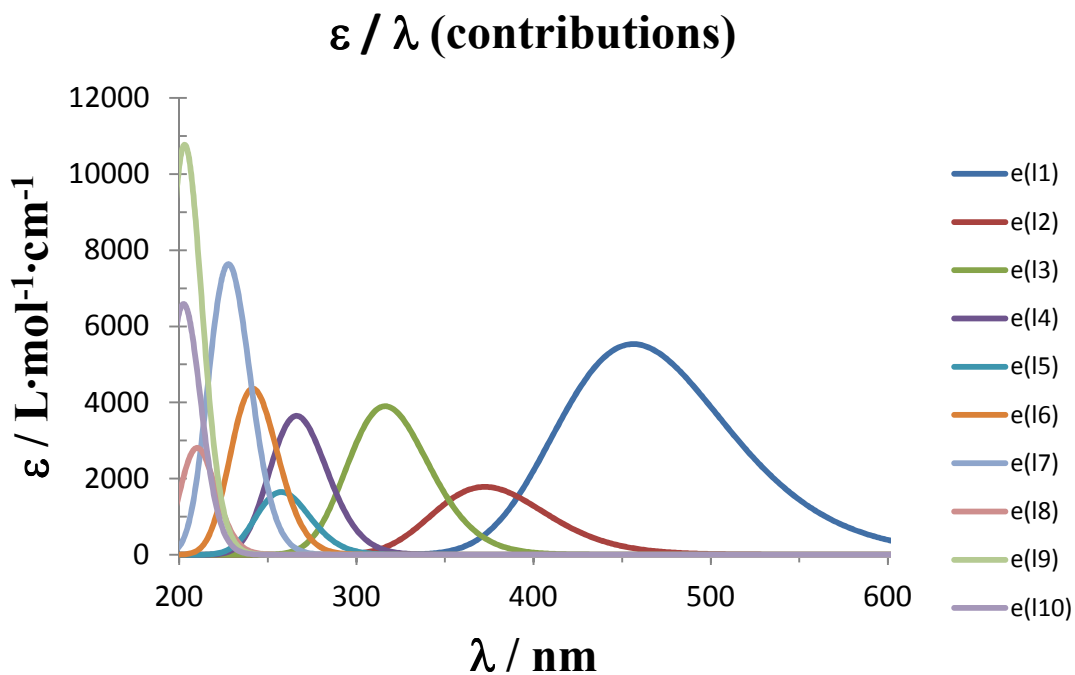


Figure 2. Contribution of relevant $S_0 \rightarrow S_n$ transitions in **1o**

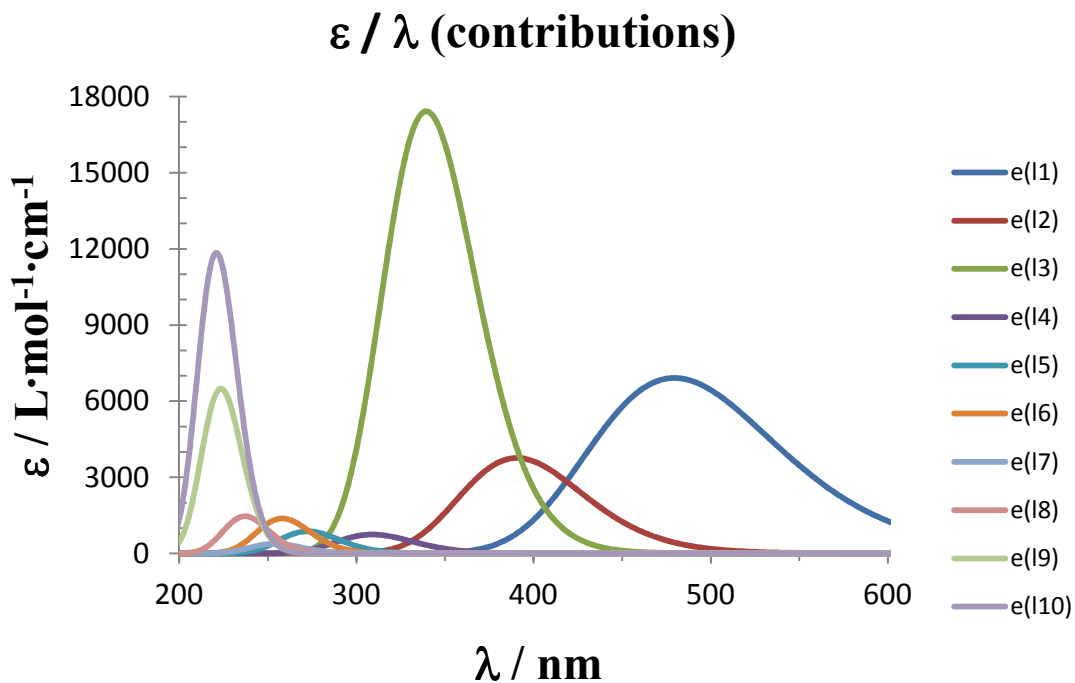


Figure 3. Contribution of relevant $S_0 \rightarrow S_n$ transitions in **1c**

The difference between the UV-VIS spectrum of the closed and open forms of **1** is illustrated in the following figure.

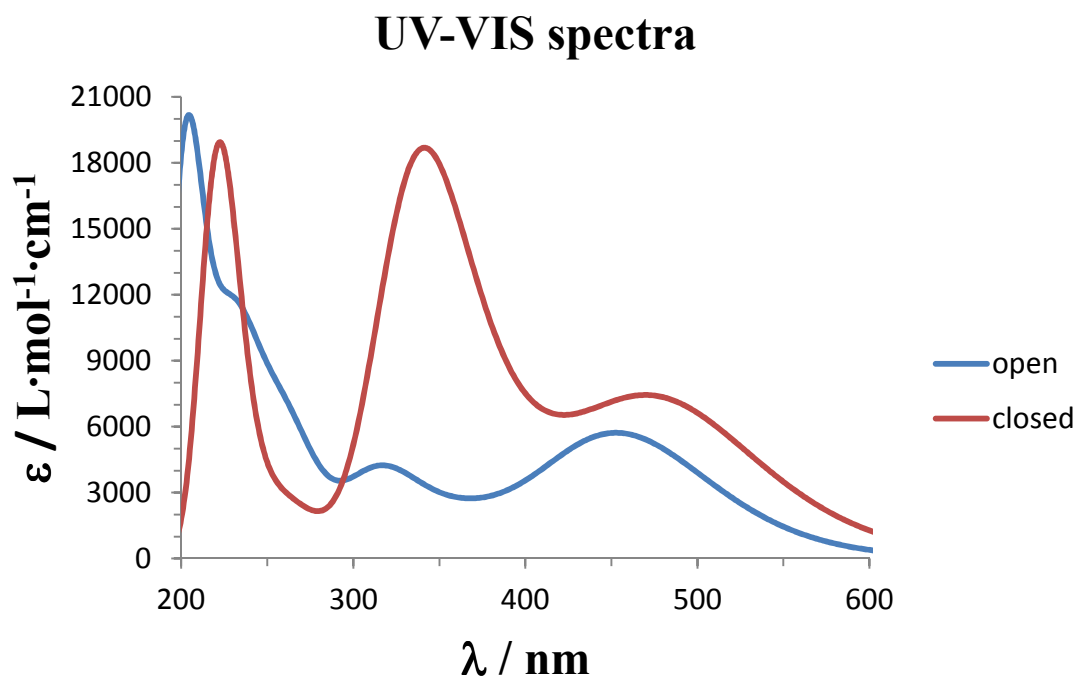


Figure 4. UV-VIS spectra of the closed and open forms of **1**

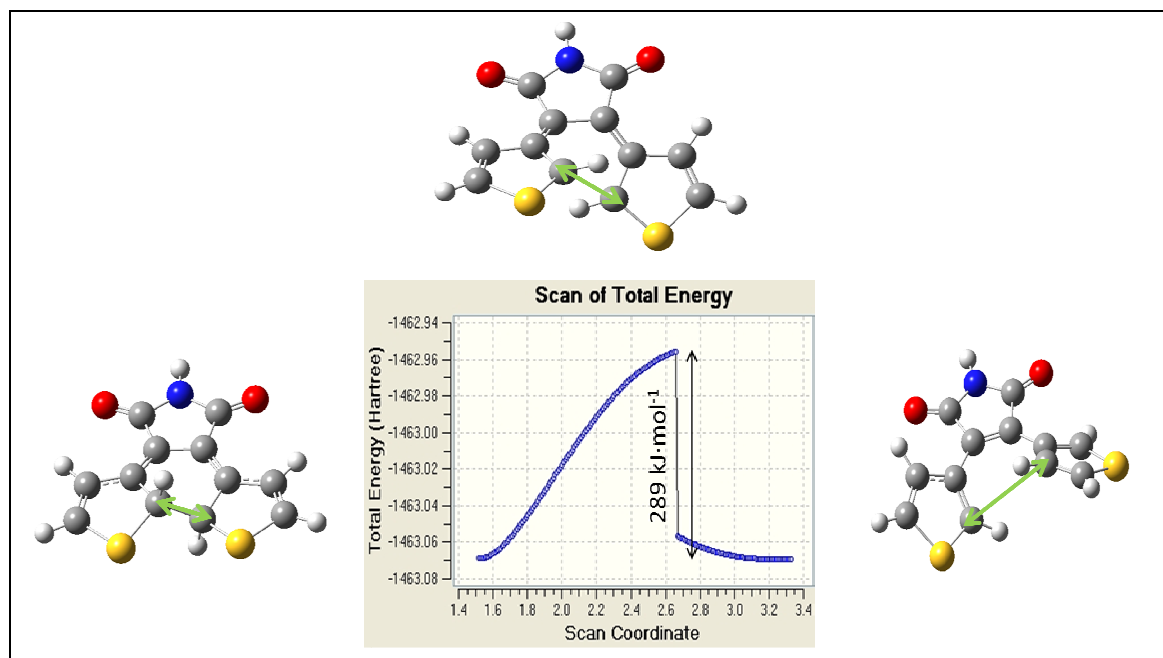


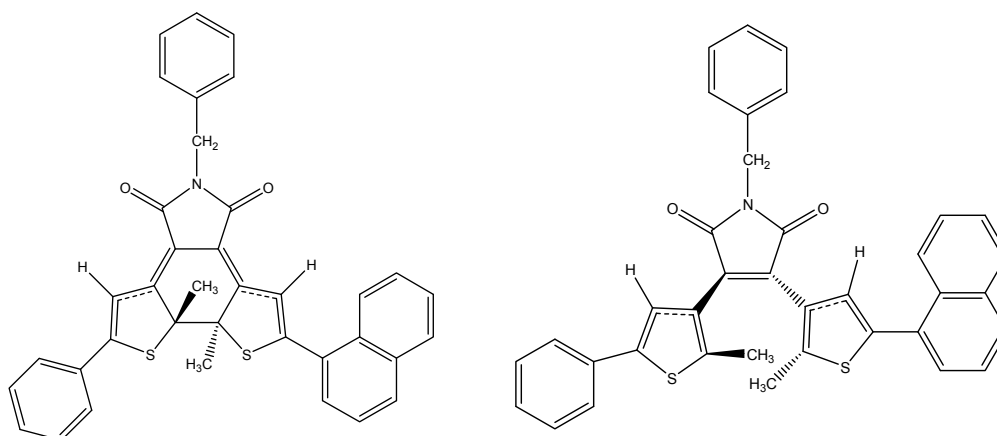
Figure 5. Scan of the C4-C15 distance in going from the closed to the open forms of **1**

All efforts to calculate a saddle point, *i.e.* a transition structure, between the stationary points corresponding to the optimized geometries of the closed and open forms of **1** were unsuccessful, which might be an indication of the photochemical nature of the closed open forms interconversion.

To get an estimation of the thermal barrier a scan calculation was carried out, the result is shown in Figure 5. The estimated barrier is $289 \text{ kJ}\cdot\text{mol}^{-1}$, *ca.* 414 nm, *i.e.* visible electromagnetic radiation of this wavelength provides enough energy for ring opening which is consistent with empiric observations.

COMPOUND 3

The next step in the theoretical understanding the behaviour of DTE compounds is the calculations involving the closed and open form of compound **3**, whose chemical structures are shown below:



The presence of three substituents relative to the model compound **1**, a phenyl group, a benzyl group and a naphthyl groups bonded at C1, N22 and C12 respectively (atom numbering is that defined for compound **1**, see Table 2) suggest a conformational study searching the lowest energy structures and the height of the conformational barriers.

The summary of the findings on the optimal conformations of the closed and open form of **3** are shown in Schemes 11 & 12 respectively.

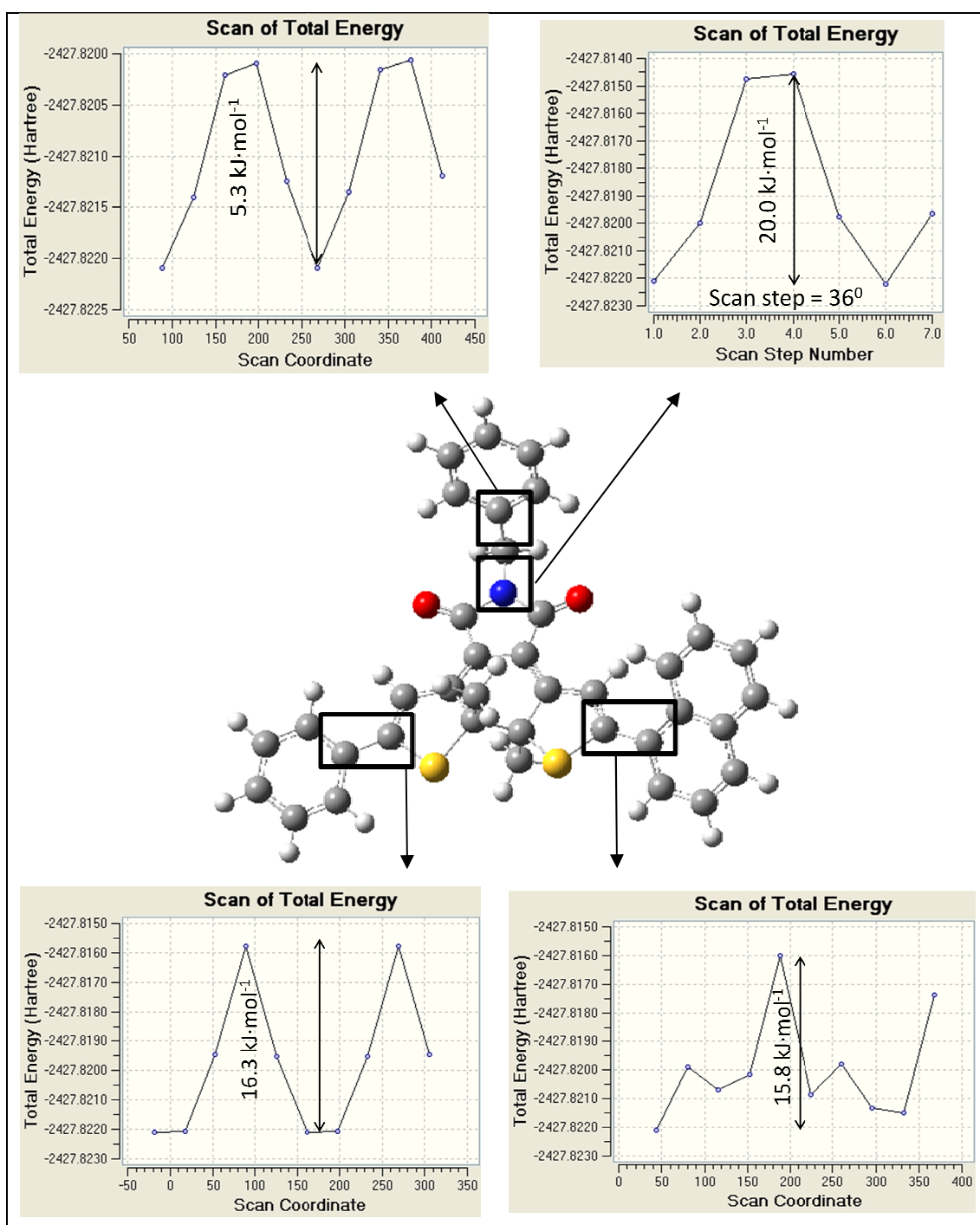


Figure 6. Conformational study of 3c

The barriers involving rotation around both bonds of the benzyl group as well as that involving the phenyl group are similar for both forms; the main difference comes from the rotation of the phenyl group, where the barrier is *ca.* $9 \text{ kJ}\cdot\text{mol}^{-1}$ higher for the open form.

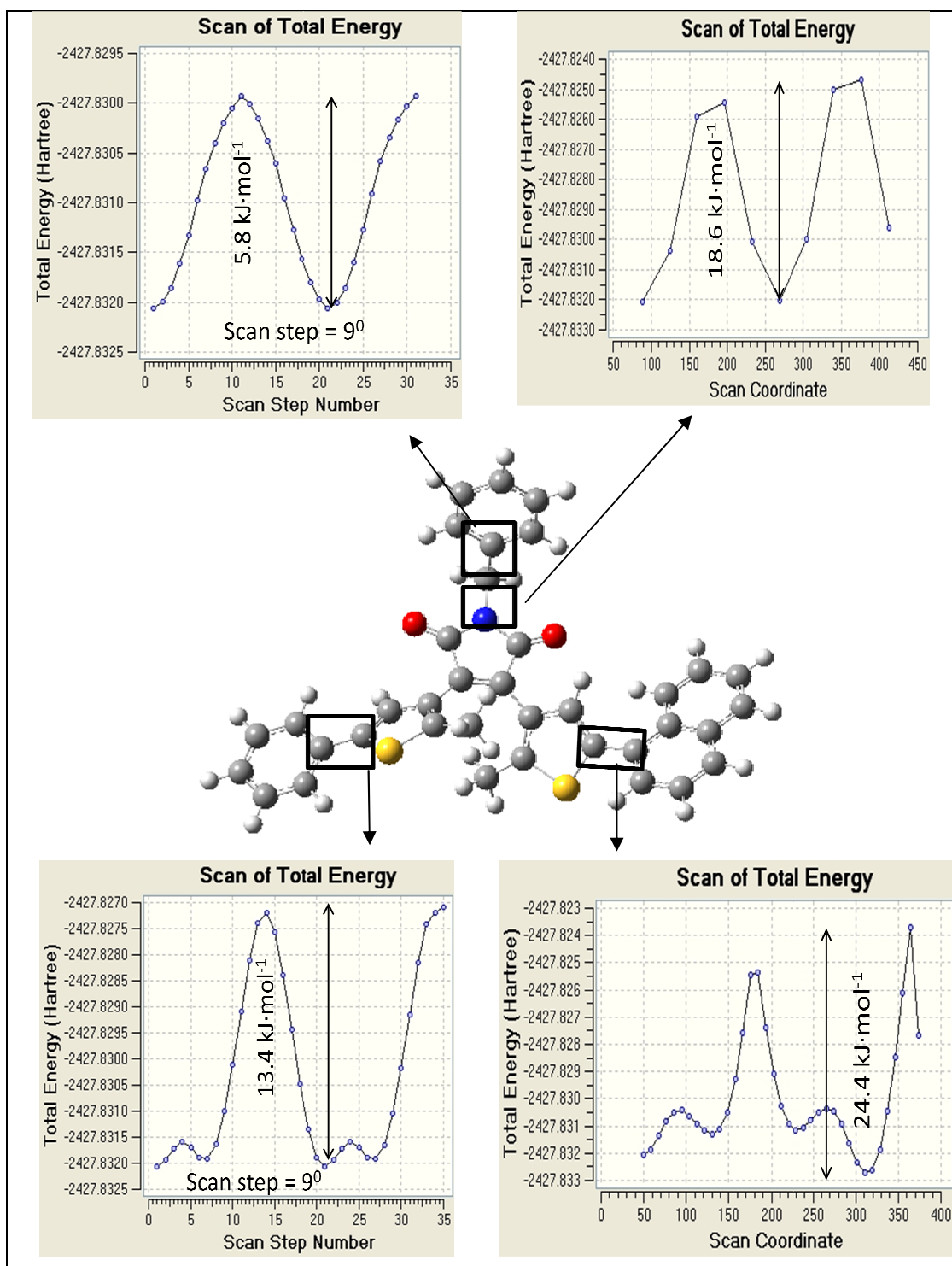
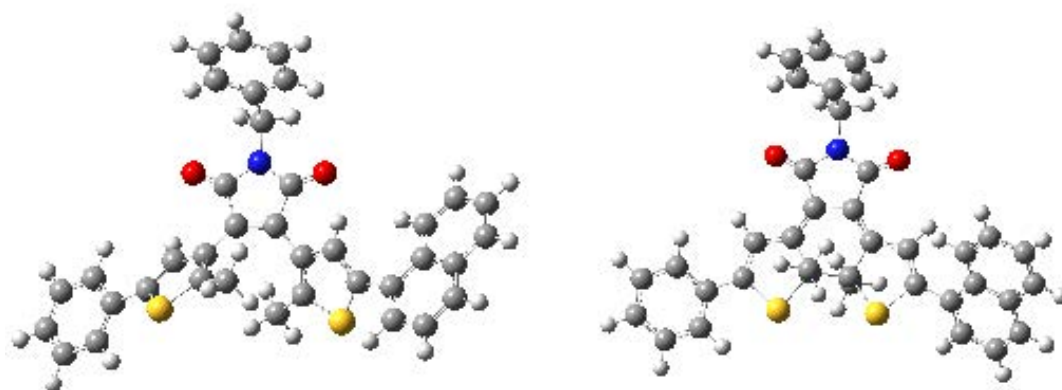


Figure 7. Conformational study of **3o**

The lowest energy conformations for the open and closed forms of compound **3** are the following:



Using those lowest energy conformations the corresponding UV-VIS spectra were calculated for the open form (Figure 8) and for the closed form (Figure 9).

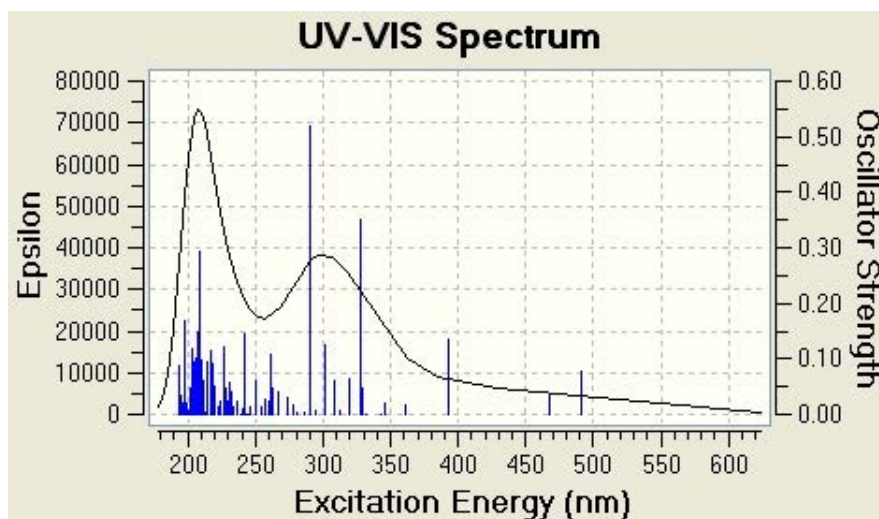


Figure 8. Calculated UV-VIS spectrum of **3o**

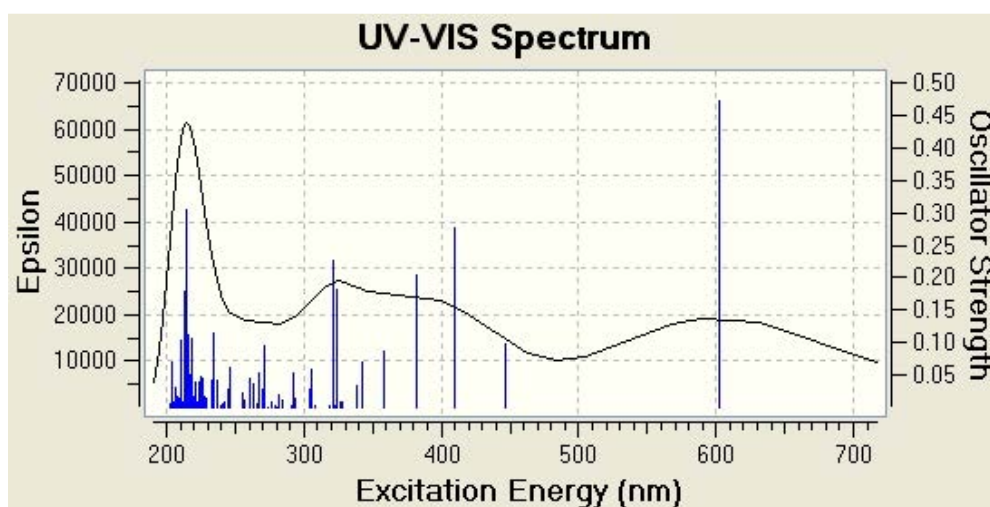


Figure 9. Calculated UV-VIS spectrum of **3c**

Table 9. Selected observed and computed wavelength maxima and molar absorptivity coefficients for compound **3o**

Experimental data	$\lambda_{\max} / \text{nm}$	293	321	410
	$\varepsilon / \text{M}^{-1}\cdot\text{cm}^{-1}$	29200	25200	5000
Calculation	$\lambda_{\max} / \text{nm}$	290	328	492
	$\varepsilon / \text{M}^{-1}\cdot\text{cm}^{-1}$	34500	24000	5000

Table 10. Selected observed and computed wavelength maxima and molar absorptivity coefficients for compound **3c**

Experimental data	$\lambda_{\max} / \text{nm}$	322	367 (sh)	387	574
	$\varepsilon / \text{M}^{-1}\cdot\text{cm}^{-1}$	31300	37500	43300	14100
Calculation	$\lambda_{\max} / \text{nm}$	320	--	386	587
	$\varepsilon / \text{M}^{-1}\cdot\text{cm}^{-1}$	24000	--	26500	19500

Tables 9 and 10 collect selected observed and computed molar absorptivity coefficients and the position of maxima of absorption for the open and closed forms of compound **3**.

Calculations reproduce reasonably well the observed absorption peaks; the main differences occur in the lowest energy absorption maximum of the open form, where they differ by 80 nm, and in the absence of a shoulder in the closed form.

Concerning molar absorptivity coefficients, calculations model properly those of the open form, whereas higher differences are found for the closed form.

SOLVENT EFFECTS

The effect of changing the solvent on the oscillator strength (f) of the two lowest singlet-singlet transitions for **1c** and **1o**, and on its equilibrium constant is collected in Table 11.

From the table it follows that the change of solvent neither modifies the value of oscillator strength nor the position of the maximum of absorption.

Table 11. Solvent effect on K_{eq} , f and λ_{abs} ($S_0 \rightarrow S_1$ and $S_0 \rightarrow S_2$) for **1**

Solvent / $K_{eq}(=closed/open)$		Form	Transition	
			$S_0 \rightarrow S_1$	$S_0 \rightarrow S_2$
Water / $1.02 \cdot 10^3$	f	closed	0.16	0.09
		open	0.13	0.05
	$\lambda_{max} /$ nm	closed	477.5	392.8
		open	456.7	371.5
Cyclohexane / $1.90 \cdot 10^3$	f	closed	0.17	0.08
		open	0.14	0.04
	$\lambda_{max} /$ nm	closed	478.8	387.5
		open	454.0	373.8
Acetone / $1.07 \cdot 10^3$	f	closed	0.16	0.09
		open	0.13	0.05
	$\lambda_{max} /$ nm	closed	478.0	392.4
		open	456.7	371.7
1,4-Dioxane / $1.80 \cdot 10^3$	f	closed	0.17	0.08
		open	0.14	0.04
	$\lambda_{max} /$ nm	closed	478.8	387.9
		open	454.2	373.6

Acetonitrile / $1.04 \cdot 10^3$	f	closed	0.16	0.09
		open	0.13	0.05
	λ_{\max} / nm	closed	477.7	392.6
		open	456.7	371.6
Dichloromethane / $1.16 \cdot 10^3$	f	closed	0.17	0.10
		open	0.13	0.05
	λ_{\max} / nm	closed	479.3	391.8
		open	456.9	372.0
Ethanol / $1.05 \cdot 10^3$	f	closed	0.16	0.09
		open	0.13	0.05
	λ_{\max} / nm	closed	478.1	392.5
		open	456.8	371.7
Carbon tetrachloride / $1.79 \cdot 10^3$	f	closed	0.17	0.08
		open	0.14	0.04
	λ_{\max} / nm	closed	479.6	388.1
		open	454.7	373.6
Chloroform / $9.06 \cdot 10^2$	f	closed	0.17	0.09
		open	0.14	0.04
	λ_{\max} / nm	closed	479.5	390.6
		open	456.3	372.5

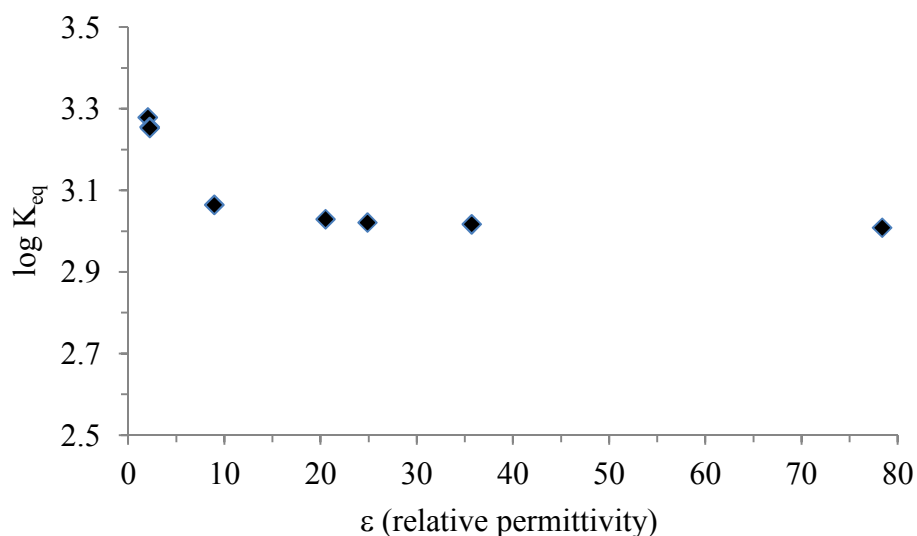


Figure 10. Effect of the polarity of the solvent on the equilibrium constant $1c \rightleftharpoons 1o$

The change of the equilibrium constant with solvent polarity is shown in Figure 10. From the figure it follows that the decrease of the solvent polarity, expressed as relative permittivity, increases the equilibrium constant, its value is twice in going from water to cyclohexane.

The effect of substituents change on the oscillator strength of the two lowest singlet-singlet transition and on the equilibrium constant of **2** and **3** is collected in Table 12.

Substitution of hydrogens for methyl groups in C4 and C15 of **1** (see atom numbering in Table 2), implies a decrease in the oscillator strength in the two lowest absorptions of both forms of **2**, and a noticeable increase in the corresponding equilibrium constant, up two orders of magnitude. Relative to **1** there is a bathochromic shift of the lowest energy maximum of absorption of the closed form, hypsochromic for the open form.

The constant of the equilibrium $3c \rightleftharpoons 3o$ is four orders of magnitude larger than that of **1** but two orders of magnitude smaller than of **2**.

The oscillator strength of the closed form of **3** (**3c**) is three fold that of **1** for $S_0 \rightarrow S_1$ transition, whereas that of the open form almost halves. For $S_0 \rightarrow S_2$ transition the value of f is similar for both forms of compounds **1** and **3**.

Table 12. Solvent effect on K_{eq} , f and λ_{abs} ($S_0 \rightarrow S_1$ and $S_0 \rightarrow S_2$) for **2** and **3**

Compound	Solvent / $K_{eq}(=closed/open)$		Form	Transition	
				$S_0 \rightarrow S_1$	$S_0 \rightarrow S_2$
2	Chloroform / $3.53 \cdot 10^9$	f	closed	0.12	0.07
			open	0.12	0.02
		$\lambda_{max} /$ nm	closed	516.9	393.7
			open	430.9	394.1
3	Chloroform / $2.16 \cdot 10^7$	f	closed	0.47	0.10
			open	0.08	0.04
		$\lambda_{max} /$ nm	closed	602.7	447.2
			open	491.6	467.9

Relative to **1** the presence of some substituents shifts the lowest energy absorption maximum to longer wavelengths for both forms, up to ca. 125 nm in the case of **3c**. All this facts are consistent with the empirical observations.

The results obtained in this work will serve the basis to carry out the computational study of the photochemistry involved in photocyclization/photoreversion reactions of dithienylethenes (DTEs).

CONCLUSIONS

CONCLUSIONES

CONCLUSIÓNS

CONCLUSIONS

Of the Computational Chemistry Study of electronic structure of DTEs [3-[thiophen-3-yl]-4-(thiophen-3-yl)-1*H* pyrrole-2,5-dione (**1**) =model compound=, [2-methylthiophen-3-yl]-4-(2-methylthiophen-3-yl)-1*H* pyrrole-2,5-dione (**2**) and 1-Benzyl-3-[2-methyl-5-(naphthalen-1-yl)thiophen-3-yl]-4-(2-methyl-5-phenylthiophen-3-yl)-1*H* pyrrole-2,5-dione (**3**)], have been obtained the next conclusions using as calculation method the functional density theory (DFT), with 6-31G(d) as basis set, and CPCM method to simulate dissolvent, mainly chloroform:

1. The central ring opening implies a substantial change in distances of carbons being broken, as well as in hydrogens attached to them. Bond angles that vary are mainly related with the central ring, and the same occurs with dihedral angles, where geometry changes are noteworthy.
2. Electronic reorganization produced by ring opening causes changes in hybridization in some atoms and also there is a noticeable charge movement in direction of the other rings.
3. The change in Gibbs free energy is going from closed to the open form indicates that the equilibrium is displaced to the open form for all the studied compounds.
4. It has not been possible to obtain any transition structure, although an estimation of energy barrier to go from the closed to the open form indicates that, according to experimental observations, the process has photochemical nature.
5. Excitation calculations reproduce reasonably well the known spectroscopic data of 1-Benzyl-3-[2-methyl-5-(naphthalen-1-yl)thiophen-3-yl]-4-(2-methyl-5-phenylthiophen-3-yl)-1*H* pyrrole-2,5-dione (**3**).
6. Changing the solvent does not implies relevant changes in oscillator strength values for the first and second excitations of both forms, either for equilibrium constant; the lower the electric permittivity fo the solvent the higher the equilibrium constant closed \rightleftharpoons open.
7. The presence of substituents increases the equilibrium constant (closed \rightleftharpoons open) several orders of magnitude.

CONCLUSIONES

Del estudio de Química Computacional de la estructura electrónica de los DTEs: [3-tiofen-3-il]-4-(tiofen-3-il)-1H pirrol-2,5-diona (**1**) =compuesto modelo=, [2-metiltiofen-3-il]-4-(2 metiltiofen-3-il)-1H pirrol-2,5-diona (**2**) y 1-bencil-3-[2-metil-5-(naftalen-1-il)tiofen-3-il]-4-(2-metil-5-feniltiofen-3-il)-1H pirrol-2,5-diona (**3**) se han obtenido las siguientes conclusiones al emplear como método de cálculo la teoría del funcional de la densidad (DFT), con 6-31G(d) como funciones base, y el modelo CPCM para simular el disolvente, principalmente cloroformo:

1. La apertura del anillo central implica un cambio sustancial en la distancia de los carbonos cuyo enlace se rompe, así como de la misma entre los hidrógenos unidos a ellos. Los ángulos de enlace que varían son principalmente los relacionados con el anillo central y lo mismo ocurre con los ángulos diedros, donde el cambio de geometría es más notable.
2. La reorganización electrónica producida al abrirse el anillo provoca no solo cambios de hibridación en diversos átomos, sino que también hay un considerable movimiento de carga hacia átomos de los otros anillos.
3. El cambio en la energía libre de Gibbs al pasar de la forma cerrada a la abierta indica que el equilibrio se desplaza hacia ésta para todos los compuestos estudiados.
4. No ha sido posible obtener la estructura de transición, si bien una estimación de la barrera energética para pasar de la forma cerrada a la abierta indica que, de acuerdo con las observaciones experimentales, el proceso puede tener lugar por activación fotoquímica.
5. Los cálculos de excitación reproducen razonablemente bien los datos espectroscópicos conocidos del 1-bencil-3-[2-metil-5-(naftalen-1-il)tiofen-3-il]-4-(2-metil-5-feniltiofen-3-il)-1H pirrol-2,5-diona (**3**).
6. Al variar el disolvente no se obtienen relevantes cambios ni en los valores de la fuerza del oscilador para las dos primeras excitaciones de ambas formas, ni tampoco en la constante de equilibrio, cuanto menor es la permitividad eléctrica del disolvente más alto es el valor de la constante de equilibrio cerrada \rightleftharpoons abierta.

7. La presencia de sustituyentes provoca un aumento de la constante de equilibrio (cerrada \rightleftharpoons abierta) de varios órdenes de magnitud.

CONCLUSIÓNS

Do estudo de Química Computacional da estrutura electrónica dos DTEs: [3-tiofen-3-il]-4-(tiofen-3-il)-1H pirrol-2,5-diona (**1**) =composto modelo=, [2-metiltiofen-3-il]-4-(2 metiltiofen-3-il)-1H pirrol-2,5-diona (**2**) y 1-bencil-3-[2-metil-5-(naftalen-1-il)tiofen-3-il]-4-(2-metil-5-feniltiofen-3-il)-1H pirrol-2,5-diona (**3**) obtivéronse as seguintes conclusións ao empregar como método de cálculo a teoría do funcional da densidade (DFT), con 6-31G(d) como funcións base, e o modelo CPCM para simular o disolvente, principalmente cloroformo:

1. A apertura do anel central implica un cambio substancial na distancia dos carbonos cuxo enlace rompese, así como da mesma entre os hidróxenos unidos a eles. Os ángulos de enlace que varían son principalmente os relacionados co anel central e o mesmo ocorre cos ángulos diedros, onde o cambio de xeometría é mais notable.
2. A reorganización electrónica producida ao abrirse o anel provoca non só cambios de hibridación en diversos átomos, senón que tamén hai un considerable movemento de carga cara átomos dos outros aneis.
3. O cambio na enerxía libre de Gibbs dende a forma pechada á aberta indica que o equilibrio desprazase cara a forma aberta para tódolos compostos estudados.
4. Non foi posible obter a estrutura de transición, se ben unha estimación da barreira enerxética para pasar da forma cerrada á aberta indica que, de acordo coas observacións experimentais, o proceso pode ter lugar por activación fotoquímica.
5. Os cálculos de excitación reproducen razoablemente ben os datos espectroscopios coñecidos do 1-bencil-3-[2-metil-5-(naftalen-1-il)tiofen-3-il]-4-(2-metil-5-feniltiofen-3-il)-1H pirrol-2,5-diona (**3**).
6. Ao variar o disolvente non se obtiveron relevantes cambios nin nos valores da forza do oscilador para as dúas primeiras excitacións de ambas formas, nin tampouco na constante de equilibrio, canto mais baixa é a permitividade eléctrica do disolvente mais alto é o valor da constante de equilibrio pechada \rightleftharpoons aberta.

7. A presenza de substituíntes provoca un aumento da constante de equilibrio (pechada \rightleftharpoons aberta) de varios ordes de magnitude.